

**Lattice-based random jammed configurations for hard particles**F. H. Stillinger,<sup>1</sup> H. Sakai,<sup>1</sup> and S. Torquato<sup>1,2</sup><sup>1</sup>*Department of Chemistry, Princeton University, Princeton, New Jersey 08544*<sup>2</sup>*Princeton Materials Institute, Princeton University, Princeton, New Jersey 08544*

(Received 5 August 2002; published 31 March 2003)

A nontrivial subset of the jammed packings for rigid disks and spheres are those that can be obtained by sequential removal of particles from periodic crystalline arrays. This paper considers the enumeration problems presented by such packings that are based on the close-packed triangular disk lattice, and the face-centered and body-centered cubic sphere lattices. Three distinct categories of packings have been distinguished, depending on their behavior with respect to nonoverlap geometric constraints and/or externally imposed virtual displacements: locally jammed, collectively jammed, and strictly jammed. Each of these possesses an upper limiting vacancy concentration beyond which no packings of the types considered can exist. For each of the three lattices, specific vacancy clusters have been identified whose presence would destroy local jamming, and some of the corresponding patterns that would destroy collective jamming in the triangular disk lattice have also been found. Within the allowable range of vacancy concentration for each case, the number of distinct jammed packings is expected to rise exponentially with system size. By using the concept of local attrition factors, approximate enumerations have been constructed for the three lattice classes of locally jammed packings. In the interests of later extension of this work, we stress that at least some aspects of these enumeration problems might benefit from the formal transcription to a lattice-gas/Ising-model representation with vacancy interactions chosen to enforce the packing category of interest.

DOI: 10.1103/PhysRevE.67.031107

PACS number(s): 62.20.Dc, 72.80.Tm

**I. INTRODUCTION**

Hard-rod, disk, and sphere models have supplied useful prototypes for a wide variety of many-body phenomena. They have also been an enduring source of many challenging theoretical problems. One class of such problems, still incompletely understood, concerns the nature of jammed packings of disks and spheres, and how the geometric details of those packings statistically depend on the choice of method by which they are created. Many of the most difficult open questions involve classification and enumeration of “random” (i.e., irregular) disk and sphere packings, and how they relate to the statistical physics of liquids, glasses, and disordered solids. Instead of attempting to resolve any of these general problems, the present study focuses on a restricted, and therefore more modest, goal: attention is confined to the statistics of the special classes of jammed packings for disks and spheres that are identifiable as vacancy-containing lattices. These selected packings (and their multicomponent relatives) may command extra attention because of their connection to known examples of radiation-damaged metals [1] and of certain types of nonstoichiometric crystals [2] both of which can contain high and variable concentrations of vacancies.

In earlier work [3] we discussed how the concept of *rigidity percolation* (which has been used to analyze the mechanical properties of network glasses) can be generalized to characterize *jammed* hard-particle packings. The standard rigidity percolation problem has been studied for lattice networks to understand the mechanical properties of network glasses [4–6]. For example, consider a triangular net of mass points connected by nearest-neighbor central forces. Such a system is stable and elastically isotropic, and is therefore characterized by  $K$  and  $G$ , the elastic moduli of compression

and rigidity, respectively. However, if bonds are randomly removed with probability  $1 - p$ , then both  $K$  and  $G$  will vanish at some  $0 < p < 1$  called the rigidity percolation threshold.

Now consider a jammed system that meets one of three definitions (locally, collectively, or strictly jammed) that we have recently introduced (see details below) [3]. Begin a process whereby particles are sequentially removed by some selection process with a random element. The applicable rigidity percolation threshold is the sphere volume fraction  $\phi^*$  at which the system ceases to be jammed according to the selected definition. Thus, the value of  $\phi^*$  will generally vary for a given starting structure, depending on the jamming category, boundary conditions, and random removal process. Unlike the standard rigidity percolation problem, applying a purely random removal process in the case of jammed particle systems will lead to a trivial result in the infinite-system limit, namely, a vacancy concentration of zero for unjamming. This behavior is explained in Sec. V below; it can be illustrated by considering first a fully dense triangular lattice of hard disks contained within an appropriately shaped finite container. This two-dimensional example is known to be strictly jammed [3], and will unjam whenever two adjacent disks are removed, i.e., no divacancies can be tolerated. For a finite system, the probability of a divacancy occurrence is less than unity at a nonzero vacancy concentration. However, in the infinite-system limit, the probability of such an occurrence approaches unity, leading to collapse (unjammed) at any positive vacancy concentration, no matter how small. This phenomenon extends to other jammed lattices and to higher dimensions. The purpose of this paper is to begin to examine modification of the removal process and its consequences for certain regular lattices in both two and three dimensions.

The following Sec. II briefly reviews the major categories of packing definitions for hard particles that are relevant for the present study. This is followed by specification, in Sec. III, of the regular lattices in two and three dimensions to be considered, and identification of the vacancy arrangements that they can sustain while qualifying as “jammed.” For each lattice and jamming category, Sec. IV introduces the enumeration functions that arise as a result of sequential particle removal from the starting perfect lattices. Section V presents some further details of the enumeration problems, as well as an approximation method for at least some of the enumeration functions. Various conclusions as well as points requiring discussion appear in the final Sec. VI. An Appendix is devoted to the behavior of the body-centered cubic sphere packing under shear strain.

## II. JAMMING CATEGORIES

Jammed configurations of rigid rods, disks, and spheres are those which, in some appropriate interpretation, have every particle locked in place by the nonoverlap constraints imposed by neighbors. For rigid rods on a line this includes only a single trivial arrangement, periodic close packing. However, the cases of rigid disks in the plane and rigid spheres in three-space give rise to rich opportunities for diversity in jamming. Although the preponderance of jammed disk and sphere configurations lack long-range order (i.e., are amorphous), even the subsets exhibiting long-range order, of the types considered below in the following Secs. III–VI, also display considerable nontrivial diversity.

The “appropriate interpretation” alluded to above refers to distinct categories of jammed disk or sphere configurations. For present purposes we distinguish three jamming definitions, arranged here in order of increasing stringency [3].

(1) *Locally jammed.* Each particle in the system is incapable of being displaced, due to nonoverlap restrictions, provided all other particles remain fixed in position. In practice this means for disks in two dimensions that each particle must be imprisoned by at least three contacting neighbors not all located in the same semicircle, and in three dimensions each sphere must be imprisoned by at least four contacting neighbors not all in the same hemisphere. The honeycomb lattice of disks, and the diamond lattice of spheres provide concrete examples of locally jammed configurations [3].

(2) *Collectively jammed.* No subset of the particles can simultaneously be displaced, so that its members move out of contact with one another and with the remainder set. If such a simultaneous displacement were indeed possible, it could be followed by further displacements that would eventually eliminate all particle contacts and leave the system totally unjammed. Obviously any collectively jammed configuration is also locally jammed, but not the reverse. Examples are the square lattice of disks, and the simple cubic lattice of spheres, provided each is enclosed within rigid walls [3].

(3) *Strictly jammed.* Any collectively jammed configuration that, by virtue of nonoverlap restrictions, disallows all uniform nonincreasing volume deformations, is classified as

strictly jammed. These disallowed deformations include volume-preserving shear deformations. The close-packed disk (triangular) and sphere (face-centered cubic) lattices are strictly jammed [3].

It is important to specify boundary conditions in an analysis of particle jamming. Two alternatives will be considered in the following. For some purposes it is appropriate to confine the disks or spheres with rigid, impenetrable walls; the interior space defined by those walls for the present study will be a convex region bounded by straight-line or planar segments. The other option imposes periodic boundary conditions with a primitive cell of such size and shape that a portion of the perfect crystal structure of interest (composed of contacting particles) just fits with its neighboring periodic-image cells. This second choice implies that any jammed configuration of local, collective, or strict type can be freely translated without fundamentally changing its character. It should be stressed that periodic boundary conditions are less restrictive than rigid boundaries; with a given primitive cell shape, any particle motions permitted by the former are permitted by the latter, but not the reverse.

It is worth noting in passing that construction methods for amorphous jammed structures tend often to yield so-called “rattler” particles [7–10]. These are isolated single particles, or small groups of particles, trapped within a confining cage of jammed particles, but free to move within that cage. A typical scenario in two dimensions would involve a rattler within a ring of seven or eight surrounding jammed disks. None of the three jamming definitions above permit the presence of rattlers. In principle, they could always be disregarded, and attention focused entirely on their jammed surrounding matrix. However, rattlers do not occur in the context of the lattice-based jammed configurations that form the subject of the present investigation.

## III. LATTICES AND INSTABILITIES

To keep the present study within manageable bounds, we have chosen to confine attention to jammed structures that are vacancy-containing variants of just three simple crystal structures. These are the triangular (tri) disk lattice in two dimensions, and the face-centered cubic (fcc) and body-centered cubic (bcc) lattices in three dimensions. The first two are maximally close packed, the last is not. A natural choice for the primitive cell for disks with either boundary condition is a rhombus containing  $m^2$  particles in a vacancy-free arrangement; an alternative choice would be a regular hexagon, which upon housing a perfect triangular crystal would contain a number of disks equal to  $3m^2 + 3m + 1$ . The corresponding natural shapes for the primitive cell for the three-dimensional examples of course are cubic, and the particle numbers for vacancy-free filling will be  $4m^3$  and  $2m^3$  for fcc and bcc, respectively. In the following we shall confine attention just to cases in which these natural system shapes (rhombus, hexagon, cube) apply. The covering fractions (the portions of the systems inside particles) in these

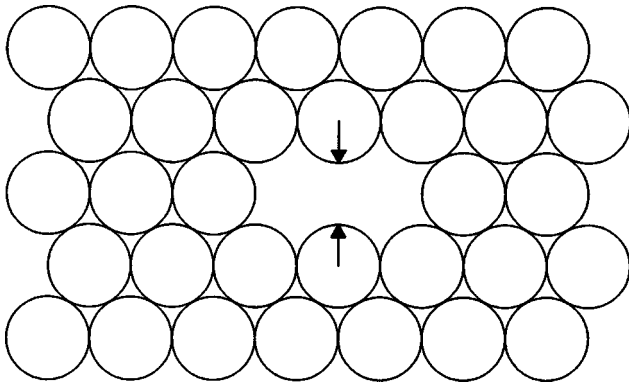


FIG. 1. Triangular lattice of contacting disks containing a divacancy. The two flanking disks above and below the divacancy are free to move inward, eliminating disk contacts, so that the system fails to satisfy the definition of a locally jammed configuration.

ideal lattices are the following:

$$\begin{aligned}\phi_{\text{tri}} &= (\pi/2)3^{1/2}, \\ \phi_{\text{fcc}} &= (\pi/3)2^{1/2}, \\ \phi_{\text{bcc}} &= 3^{1/2}\pi/8.\end{aligned}\quad (3.1)$$

Both the triangular and fcc perfect lattices are strictly jammed with either boundary condition choice. However, the bcc perfect lattice is only collectively jammed with rigid boundaries [3], a demonstration of which appears in the Appendix, and only locally jammed under periodic boundary conditions.

If a single disk is removed from an initially complete triangular lattice of  $N$  disks, thus forming a monovacancy, the six disks that were the nearest neighbors of the one removed have their coordination numbers reduced from six to five. Nevertheless, the system with the monovacancy is still locked into a strictly jammed configuration, able only to move as a whole across periodic boundaries that may have been imposed. The same comment also applies if a second disk is removed from the system, provided that its location is remote from that of the first removal, i.e., if the system is composed of  $N-2$  disks and two monovacancies. However, if the second disk removed is one of the six neighbor particles of the first monovacancy, the result is a divacancy as shown in Fig. 1. This divacancy structure does not even meet the local jamming criterion, as inspection of the figure immediately shows, because either of the two remaining disks at the sides of the divacancy is free to move inward. Such a displacement can be followed by a sequence of others that eventually could eliminate an arbitrarily large number of disk contacts. Alternatively, a sequence of disk displacements of step length equal to a diameter can move the divacancy anywhere throughout the crystal, and such motions can be used to effect arbitrary permutations of disk locations.

Similarly, one or more isolated monovacancies contained within fcc or bcc structures do not alter their jamming characters (strict, and collective or local, respectively). The particles flanking a monovacancy (12 for fcc, 8 for bcc) are

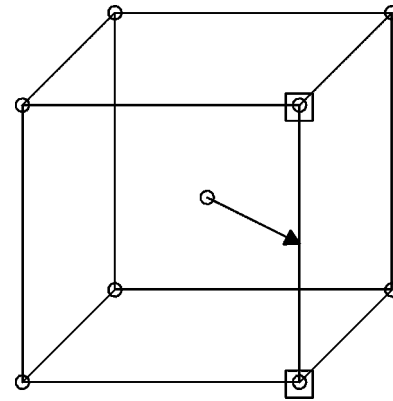


FIG. 2. Local instability in a bcc structure created by a missing pair of spheres that are second neighbors to one another. Four spheres flanking this double vacancy (symbolized by small squares) are free to move, one of which is shown here, with its direction of uninhibited displacement toward the center of the double vacancy indicated by the arrow. For ease of visualization, only sphere centers are indicated, as small circles.

missing a neighbor to be sure, but those that remain suffice to prevent any local rearrangements, either singly or collectively (depending on boundary conditions). But in contrast to the two-dimensional triangular disk lattice, a divacancy formed by removal of a pair of nearest-neighbor spheres is also incapable of altering the jamming character of either of these three-dimensional packings. However, there is an important distinction between the fcc and bcc cases. Removing a pair of spheres that are second neighbors from the fcc lattice does not change its jamming characteristic, but the same is not true for the bcc structure. As Fig. 2 illustrates, the presence of a bcc pair of second-neighbor vacancies frees four flanking spheres to move inward toward the center of that missing pair, so that the resulting configuration is not even locally jammed. More widely separated pairs of monovacancies in the bcc case do not produce equivalent local instabilities.

The smallest vacancy cluster in the fcc structure that can destroy its jamming character is a compact trivacancy. This results from removal of three spheres which were mutual nearest neighbors, i.e., which formed an equilateral triangle. Such a compact trivacancy borders one unremoved sphere, to one or the other side of its plane, which is free to move into the cluster. In a fashion analogous to that of the triangular disk lattice containing a divacancy, a sequence of sphere hops into the trivacancy has the effect of moving it throughout the entire system, while permuting sphere positions in its wake. Trivacancies that are formed by removal of a linear triad of contacting spheres, or a triad with a  $2\pi/3$  or a  $\pi/2$  bend, do not alter the jamming character of the fcc lattice. It should be noted in passing that extended vacancy “tunnels,” with direction changes and branching, apparently can exist as stable features within a locally, collectively, or strictly jammed fcc system.

Although it is relatively easy to decide whether a given vacancy-containing lattice structure meets, or fails to meet, the local jamming criterion, it is generally a more challenging task to decide if a locally jammed configuration also

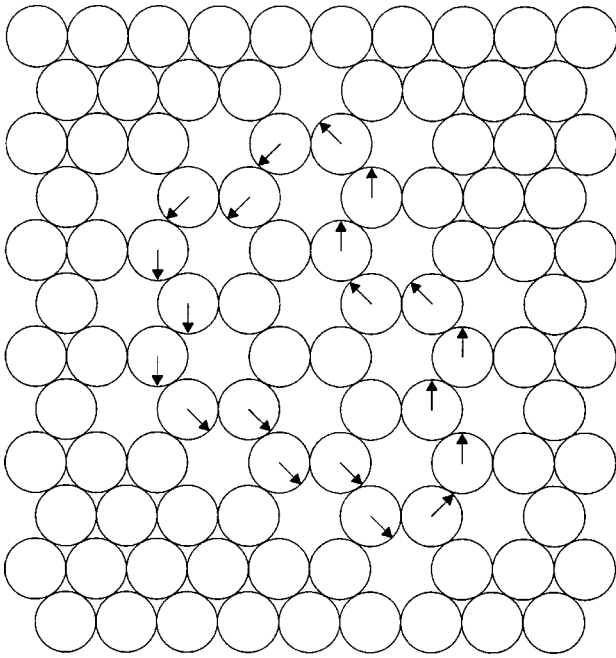


FIG. 3. Portion of a locally jammed disk configuration, based on the triangular lattice, which contains a collective instability. A closed circuit of simultaneous disk displacements has been indicated by arrows, the effect of which would be to eliminate disk contacts that are necessary for jamming.

satisfies the collectively jammed or even the strictly jammed criteria [3]. However, in the case of the triangular disk lattice confined by rigid boundaries in either the rhombus or hexagon form, a straightforward, if cumbersome, test can be applied to tell whether a locally jammed configuration is also collectively jammed. The principle involved is illustrated in Fig. 3, where a specific collective displacement of several disks around a closed path, uninhibited by disk repulsions, has been identified that would eliminate disk contacts and destroy jamming. All such collective displacement paths display the following features.

(a) Each disk serving as a vertex of the path is a point at which the path changes direction by  $\pm\pi/3$ .

(b) Each disk of the path in its undisplaced position contacts exactly three disks, two that are fore and aft along the path, and one not part of the path. The last may be on either side of the path, but in every case is opposite the  $2\pi/3$  bend angle at the path vertex.

The smallest such path is the regular hexagon. Although it is not true in every instance, any larger path, such as that shown in Fig. 3, may contain within it one or more of these small hexagonal paths that by themselves can act as displacement cycles. Examination of Fig. 3 reveals several of these.

**IV. GENERATION AND ENUMERATION PROBLEMS**

The obvious approach to generating the packings discussed above is to start with a complete and perfect lattice, and then to remove disks or spheres sequentially, subject to a suitably chosen protocol. If the objective is to form and to enumerate packings that are at least locally jammed, it would

suffice to use a random selection of particles present for removal, subject to the constraint that “dangerous” vacancy clusters, such as those identified in the preceding Sec. III, are not permitted to occur. These include the divacancy for the triangular disk lattice, the equilateral triangular trivacancy for the fcc sphere lattice, and the next-nearest-neighbor double vacancy for the bcc sphere lattice.

Suppose that before any particle removal, the primitive cell for the lattice of interest contained a large number  $N$  of disks or spheres. Some number  $n$  of these will be removed. Let  $\Omega_\alpha(N,n)$  stand for the number of *distinguishable* jammed packings that can result, where the index  $\alpha=l,c,s$  indicates, respectively, the type under consideration: at least locally, at least collectively, or strictly jammed. Recall that we consider both rigid boundary conditions, as well as periodic boundary conditions. Only the latter have the possibility of freely translating any configuration to an alternative position by any multiple of the lattice basis vectors. Consequently, for all three lattices and for all three  $\alpha$  choices, we have

$$\Omega_\alpha(N,0) = 1,$$

$$\Omega_\alpha(N,1) = N \quad (\text{rigid boundary conditions}), \quad (4.1)$$

and

$$\Omega_\alpha(N,0) = \Omega_\alpha(N,1) = 1 \quad (\text{periodic boundary conditions}). \quad (4.2)$$

The enumeration quantities  $\Omega_\alpha$  can only be nonzero for some range of the integer variable  $n$  that will depend on the lattice chosen, the jamming category  $\alpha$ , and the boundary conditions. The upper limit for this variable is determined by the least-dense jammed packing of type  $\alpha$ . As an example, consider the triangular disk lattice. If local jamming is the category of concern, the least-dense structure in the large-system limit will be dominated by the pattern of the honeycomb lattice, illustrated in Fig. 4. This structure has coordination number equal to three, and consists entirely of rotatable hexagons of disks. It is important to bear in mind that this pattern may have to be broken at a rigid boundary to preserve the local jamming criterion, but this is only a “surface” correction; and with periodic boundary conditions the honeycomb pattern might be out of phase with its images, thus also requiring a “surface” modification. One-third of the disks are missing from the precursor triangular lattice to form the extended honeycomb structure, so that in this case the large-system asymptotic upper limit to the number of vacancies will be given by

$$n_{\max} \sim N/3 \quad (\text{tri, local jamming}). \quad (4.3)$$

The more stringent requirement to have at least collective jamming cannot tolerate the low disk density implied by Eq. (4.3), but instead terminates at a higher disk density (lower vacancy number). In the large-system limit this is illustrated by the Kagomé lattice pattern, Fig. 5, for which the coordination number is four. With periodic boundary conditions, it does not quite suffice to have the perfect Kagomé structure



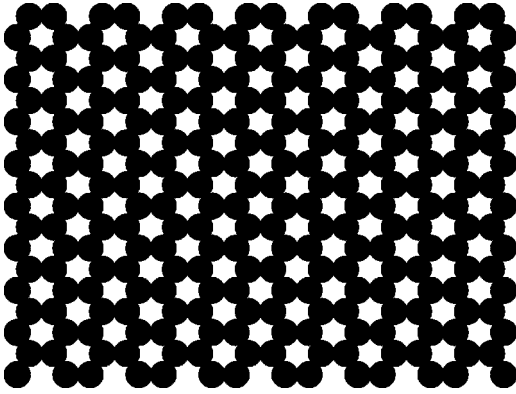


FIG. 4. Honeycomb lattice of contacting disks. This is the lowest-density structure related to the triangular disk lattice that remains locally jammed.

everywhere throughout the system. But if two nonparallel principal rows of vacancies in this structure are refilled all the way across the system, this just manages to produce collective jamming. In the large-system limit, such refilling of two rows represents a negligible change in the vacancy concentration from that of the perfect Kagomé lattice, so we have

$$n_{\max} \sim N/4 \quad (\text{tri, collective jamming}). \quad (4.4)$$

However the Kagomé structure is not unique in this respect. The pattern of vacancies in the Kagomé lattice can be altered from triangular to rectangular, as shown in Fig. 6. The resulting structure continues to exhibit coordination number four. It also satisfies Eq. (4.4), provided that it similarly has had two nonparallel principal rows of vacancies refilled. With respect to stacking periodicity in the vertical direction in Figs. 5 and 6, these alternatives (in their perfectly periodic forms) are analogous respectively to the three-dimensional face-centered cubic and hexagonal close-packed structures. It must also be noted that two-row refilling not only produces collective jamming for these two

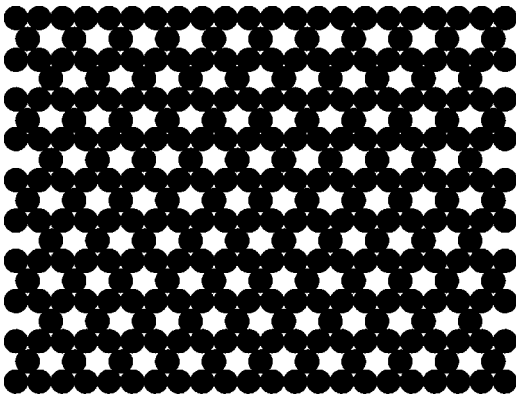


FIG. 5. The Kagomé lattice of contacting disks. Provided that rigid boundaries are present, this structure attains the lowest particle density for collectively jammed structures based on the triangular lattice.

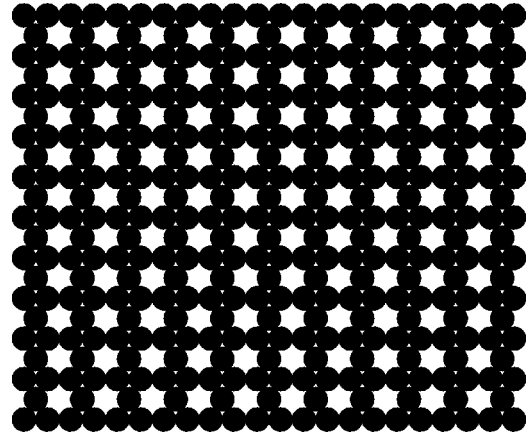


FIG. 6. Collectively jammed disk packing created by converting the triangular vacancy array of the Kagomé lattice (Fig. 5) to a rectangular array. This conversion leaves the density and coordination number unchanged.

structures, but simultaneously converts both of these cases to the more stringent category of strict jamming. Consequently, we also have

$$n_{\max} \sim N/4 \quad (\text{tri, strict jamming}). \quad (4.5)$$

Limits on the vacancy contents for the three-dimensional lattices also exist, but are more difficult to find. However, some results can be stated. The fcc lattice consists of four equivalent interpenetrating simple cubic lattices. If all spheres comprised in one of these sublattices are removed, the result is still a strictly jammed structure with either choice of boundary conditions. Consequently, we have

$$n_{\max} \geq N/4 \quad (\text{fcc, strict jamming}). \quad (4.6)$$

In addition, the bcc lattice consists of two equivalent interpenetrating diamond lattices. If one of these two is removed, the remaining diamond lattice is only locally jammed, but because each of its spheres has the minimal coordination number (four) for local jamming, it cannot tolerate any further sphere removals. Therefore

$$n_{\max} = N/2 \quad (\text{bcc, local jamming}). \quad (4.7)$$

## V. ENUMERATION VERSUS DENSITY

Although each of the specific examples just cited involves a periodic structure, the fact remains that, over each of the ranges  $0 \leq n \leq n_{\max}(\alpha)$ , the great majority of the packings enumerated by the functions  $\Omega_{\alpha}(N, n)$  will contain irregular, nonperiodic arrangements of vacancies. One of the basic tasks, then, is to calculate, or at least to approximate, these enumeration functions. We shall continue to be interested in the large-system limit, for which the fractional concentration of vacancies

$$x = n/N \quad (5.1)$$

is an appropriate intensive variable. In that large-system limit,  $x$  can be treated substantially as a continuous variable over its range of definition. Furthermore, one expects each  $\Omega_\alpha$  in the same asymptotic limit to behave as follows:

$$\ln[\Omega_\alpha(N, n)] \sim N\sigma_\alpha(x). \quad (5.2)$$

This result emerges from the expectation that  $\Omega_\alpha$  in a large system should be asymptotically multiplicative over its (large) subsystems. A standard thermodynamic interpretation identifies each  $\sigma_\alpha$  as a configurational entropy per site divided by Boltzmann's constant  $k_B$ .

Let us confine attention for the moment to the local jamming criterion ( $\alpha=1$ ). Under the frankly unrealistic assumption that at given  $N, n$  the particles and vacancies could randomly intermix, one would obtain an upper bound for  $\Omega_\alpha(N, n)$ , namely,

$$\Omega_\alpha(N, n) \leq \frac{N!}{n!(N-n)!}, \quad (5.3)$$

or equivalently for the large-system limit

$$\sigma_1(x) \leq -x \ln x - (1-x) \ln(1-x) \quad [0 \leq x \leq x_{\max}(l)]. \quad (5.4)$$

This disregards the occurrence of "unjammed" vacancy clusters such as those identified in the preceding Sec. IV for each of the lattices. However, such clusters are statistically infrequent for very small  $x$ , and so the upper bound (5.4) should be tight in that regime. But as  $x$  increases toward its upper limit for the lattice of interest, the bound necessarily becomes poorer as random occurrence of pairs of vacancies that are placed next to one another becomes an increasingly likely local pattern. This situation, and its system-size-dependent implications, can be illustrated by a series of straightforward computer simulations. Using a pseudoran-

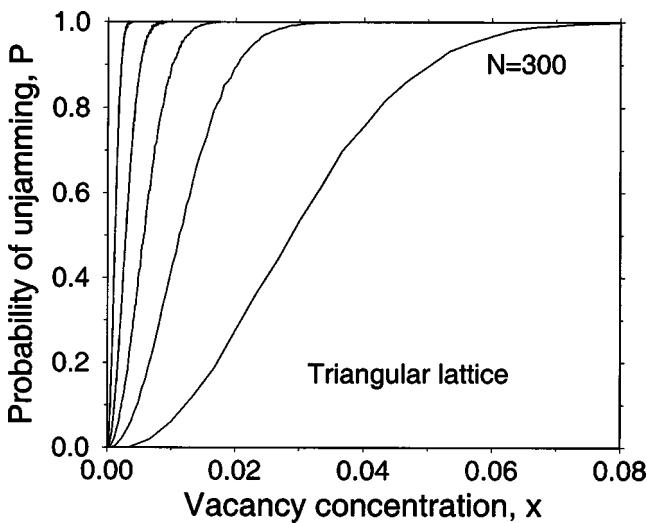


FIG. 7. Probabilities that triangular disk lattice systems, with unconstrained random disk removals, remain locally jammed as a function of the vacancy concentration. The numbers  $N$  of disks in the starting complete lattices (right to left in the figure) are 300, 1875, 7500, 30 000, and 187 500.

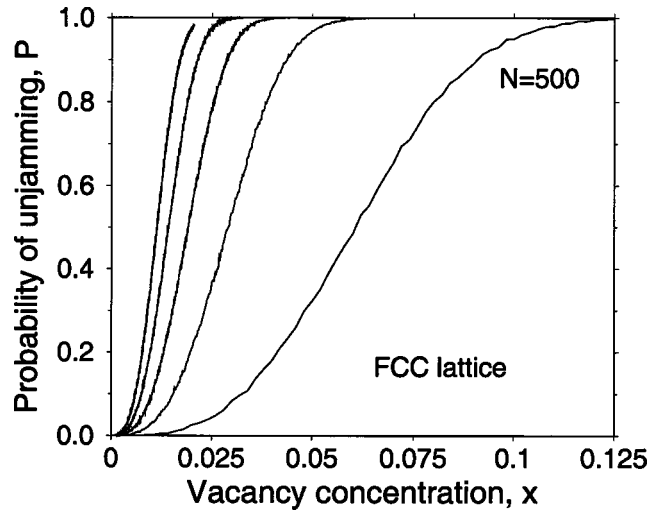


FIG. 8. Probabilities that fcc sphere lattice systems, with unconstrained random sphere removals, remain locally jammed as a function of the vacancy concentration. The numbers  $N$  of spheres in the starting complete lattices (right to left in the figure) are 500, 4000, 13 500, 32 000, and 62 500.

dom number generator to select particles for successive removal (without constraint) from a set of reasonably large lattices, it is possible to test whether the resulting configuration at each stage of removal remains locally jammed, using the geometric criteria described in the previous Sec. III. Figure 7 presents a set of results for triangular disk lattices of several sizes, subject to periodic boundary conditions, specifically indicating as a function of  $x$  how the probability of becoming locally unjammed increases monotonically as particles are sequentially removed. Figures 8 and 9 do the same for the fcc and bcc cases, respectively. Each of the curves shown in Figs. 7–9 represents an average of 10 000 separate runs of unconstrained random particle removal.

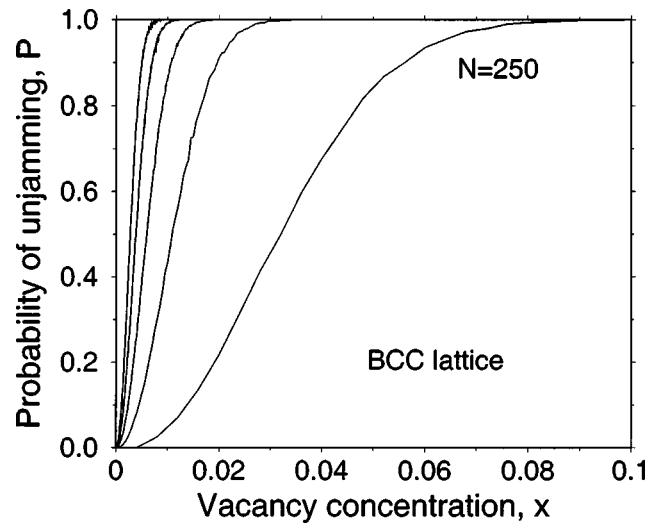


FIG. 9. Probabilities that bcc sphere lattice systems, with unconstrained random sphere removals, remain locally jammed as a function of vacancy concentration. The numbers  $N$  of spheres in the starting complete lattices (right to left in the figure) are 250, 2000, 6750, 16 000, and 31 250.

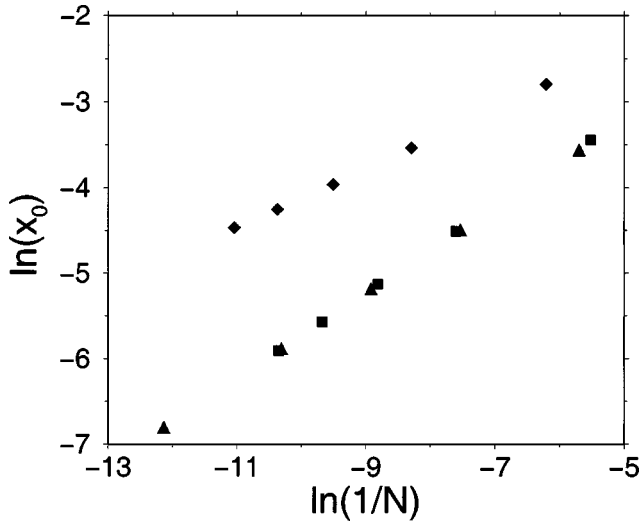


FIG. 10. Plots of  $x_0$ , the positions of vertical midpoints for the families of curves appearing in Figs. 7–9. The triangular lattice case is denoted by diamonds, the bcc case by squares, and the fcc case by circles.

The system-size scaling of the families of curves in Figs. 7–9 can be inferred from an elementary argument. For the triangular disk lattice consisting of  $N$  sites, the number of nearest-neighbor site pairs that could become a divacancy is  $3N$ . But with random deletion of particles from sites at stage  $x$ , the expected number of divacancies is  $3Nx^2$ . Choosing

$$x = (3N)^{-1/2} \quad (5.5)$$

sets this expectation value equal to unity, which corresponds to equal probabilities for local jamming and for unjamming. This in turn corresponds to the vertical-direction midpoint of the curves in Fig. 7. Exactly the same expression (5.5) applies to the expectation value unity for the number of double vacancies on second-neighbor sites in the bcc case. For the fcc lattice,  $6N$  is the number of compact triangles that could serve as trivacancy sites, to eliminate local jamming. Because the expected number of such trivacancies is  $6Nx^3$ , expectation value unity and the vertical-direction midpoints of the fcc curves in Fig. 9 correspond to

$$x = (6N)^{-1/3}. \quad (5.6)$$

Figure 10 presents plots of the vertical-direction midpoint locations, denoted by  $x_0$ , for all of the curves in Figs. 7–9, versus  $\ln(1/N)$ . Just as Eqs. (5.5) and (5.6) indicate, the triangular and bcc cases lie on a straight line with slope  $1/2$ , while the fcc results lie on another straight line with slope  $1/3$ .

We now develop an approximation procedure for the three  $\sigma_l(x)$  functions. This approximation is analogous to the one invoked by Pauling many years ago to estimate the residual entropy of ice [11,12]. The unconstrained random-mixing expression that appeared in the right member of inequality (5.3) neglected the possible occurrence of vacancy arrangements in the first-neighbor shell of any remaining particle that would be inconsistent with local jamming. Denote by

$f(x)$  the fraction of neighbor occupancy states, each weighted appropriately by the proper powers of  $x$  and of  $1-x$ , that in fact are consistent with local jamming. Realizing that one such attrition factor might be considered for each remaining particle, inequality (5.3) becomes replaced by the improved estimate

$$\Omega_l(N, n) \cong \left[ \frac{N!}{n!(N-n)!} \right] [f(x)]^{N-n}, \quad (5.7)$$

and so

$$\sigma_l(x) \cong -x \ln x + (1-x) \ln [f(x)/(1-x)]. \quad (5.8)$$

We stress that this approach assumes independence (no correlation) among attrition factors, an approximation that is subject to improvement in a more sophisticated analysis.

The *a priori* occurrence probabilities of 0, 1, ..., 6 vacancies in the first-neighbor shell of a disk in the triangular lattice are given, respectively, by the terms in the expression

$$(1-x)^6 + 6(1-x)^5x + 15(1-x)^4x^2 + 20(1-x)^3x^3 + 15(1-x)^2x^4 + 6(1-x)x^5 + x^6 \equiv 1. \quad (5.9)$$

Some of the configurations represented by these terms are inadmissible for local jamming. Only nine of 15 cases of two vacancies are admissible, only two of 20 cases of three vacancies, and none with four, five, or six vacancies are admissible. As a result, the corresponding polynomial representing the weighted numbers of local-jamming-acceptable configurations is

$$(1-x)^6 + 6(1-x)^5x + 9(1-x)^4x^2 + 2(1-x)^3x^3 \equiv (1-x)^3(1+x)(1+2x-2x^2). \quad (5.10)$$

This polynomial is the desired attrition factor  $f(x)$  for each occupied site. Substitution into Eq. (5.8) yields

$$\sigma_{\text{tri},l}(x) \cong -x \ln x + (1-x) \ln [(1-x)^2(1+x) \times (1+2x-2x^2)]. \quad (5.11)$$

Numerical investigation shows that this expression remains non-negative over the permissible range  $0 \leq x \leq 1/3$ , while exhibiting a single maximum at which

$$x \cong 0.1989, \quad (5.12)$$

$$\sigma_{\text{tri},l}(0.1989) \cong 0.332826.$$

By definition, these last results locate (at least approximately) the concentration of vacancies that produces the greatest number of locally jammed packings, and specify the exponential growth rate of that number with increasing system size. It should be noted in passing that the approximate expression (5.11) remains positive as  $x \rightarrow 1/3$ , although the exact behavior requires that it vanish in that limit.

Similar arguments can be applied to the bcc and fcc lattice cases. The result for the enumeration function  $\sigma_{\text{bcc},l}$  is found to be the following:

$$\sigma_{\text{bcc},l}(x) = -x \ln x + (1-x) \ln[(1-x)^3(1+4x-2x^2-4x^3+3x^4)]. \quad (5.13)$$

This function has its maximum within the allowable range  $0 \leq x \leq 1/2$  at the following position:

$$x \cong 0.1307, \\ \sigma_{\text{bcc},l}(0.1307) \cong 0.241827. \quad (5.14)$$

In view of the fact that the approximation (5.13) becomes negative for  $x > 0.3430$ , whereas it should remain non-negative for all  $x < 1/2$ , it is tempting to conclude that Eq. (5.13) is actually a lower bound to the exact bcc result.

The 12 neighbors of any sphere in the fcc lattice have centers located at the vertices of a polyhedron with 14 faces. Eight of these faces are equilateral triangles, the remaining six are squares. Removing the particles of either type of face to create a compact trivacancy or square tetravacancy, respectively, leaves the remaining nine or eight neighbors localized in one hemisphere about the central sphere. Consequently, either type of face removal results in a violation of the local jamming status, and so must be avoided. Subject to this understanding, systematic examination of all possible arrangements of spheres and vacancies among the 12 neighbor sites in the fcc lattice finally yields the following result for that structure:

$$\sigma_{\text{fcc},l}(x) \cong -x \ln x + (1-x) \ln[(1-x)^3(1+4x+10x^2+12x^3-3x^4-12x^5-12x^6+6x^8)]. \quad (5.15)$$

Once again this exhibits a single positive maximum, located at

$$x \cong 0.2615, \\ \sigma_{\text{fcc},l}(0.2615) \cong 0.468500. \quad (5.16)$$

The expression (5.15) remains positive over the rather wide interval  $0 < x < 0.6142$ , perhaps indicating that in this case the attrition-factor approximation has yielded an upper bound to the exact function. In this connection, it has been determined [13] that random removal of spheres from the fcc lattice, subject only to the compact-triangle-avoidance constraint, can produce strictly and, hence, locally jammed structures with  $1-x$  as low as 0.70. Possibly a more carefully patterned vacancy arrangement would produce a yet lower  $1-x$  value.

## VI. CONCLUSIONS AND DISCUSSION

Providing a complete statistical description and enumeration of all jammed packings for rigid disks and for spheres constitutes a daunting task. The present investigation has identified and focused instead on a more manageable objective, specifically the examination of jammed packings that arise from particle removals from the close-packed triangular lattice (disks), and from the face-centered and body-centered cubic lattices (spheres). Three categories of jammed pack-

ings have been distinguished: locally jammed, collectively jammed, and strictly jammed. Upper limits on the vacancy concentrations for each category have been identified, as well as some of those vacancy-cluster configurations that would violate the jamming classification. Using the notion of particle-environment attrition factors, we have derived approximate local jamming enumeration functions of vacancy concentration for the three lattices, and in each case a single enumeration (entropy) maximum appears as a function of that vacancy concentration.

The vacancy set for any depleted lattice can be viewed as an example of the venerable “lattice gas” family of models that has a rich tradition in statistical mechanics, especially due to the formal connection to spin-1/2 Ising models [14–16]. The vacancy-cluster constraints that must be observed to comply with local, collective, or strict jamming can be interpreted as interactions operating among the vacancy “particles” of the lattice gas. The case of local jamming in the triangular disk lattice is especially simple, wherein nearest-neighbor pairs of vacancies experience infinite repulsion, but are noninteracting at all other pair separations. Local jamming in the bcc lattice requires infinite repulsive pair interactions for second-neighbor pairs of vacancies, but no other interactions (including first-neighbor pairs). All vacancy pairs are interaction-free for the locally jammed fcc case, but compact equilateral triangles of vacancy triplets (mutual nearest neighbors) must be prevented by infinite three-body interactions, and square tetravacancies must be prevented by infinite four-particle interactions. The vast array of methods that have been developed in the past to handle lattice-gas and Ising models [14–16] offers opportunities for improving upon the approximate attrition-factor results described in the preceding Sec. V for local jamming enumeration. We hope to exploit these opportunities in the near future.

In connection with the lattice-gas interpretation, we note in passing that a generalization suggests itself which may be instructive to pursue at some stage. Specifically, one can restrict the occurrence of vacancies to greater pair distances, and again pose the same kind of enumeration questions as above in that extended situation. As an example, consider the triangular lattice, and impose the constraint that vacancies can exist no closer to one another than at fourth-neighbor positions. It is interesting to note that the maximum vacancy concentration permitted by this demand is  $x_{\text{max}} = 1/7$ , and that this maximum is attained in a periodic chiral structure. Figure 11 illustrates one of the mirror-image pair of patterns. This disk packing is strictly jammed with either rigid-wall or periodic boundary conditions.

Collective and strict jamming constraints in principle also lend themselves to transcription into lattice-gas interactions. However, such interactions will have arbitrarily high orders in “particle” number, and consequently may be essentially useless for computational or analytic purposes.

For small values of  $x$ , Eq. (5.1), typical system configurations under local, collective, or strict jamming protocols will exhibit no long-range order in the arrangement of vacancies. But when  $x$  rises to its maximum in each case, the resulting vacancy patterns indeed display long-range periodic order, as Figs. 4, 5, 6, and 11 have illustrated. This raises the basic question, for each lattice and jamming cat-



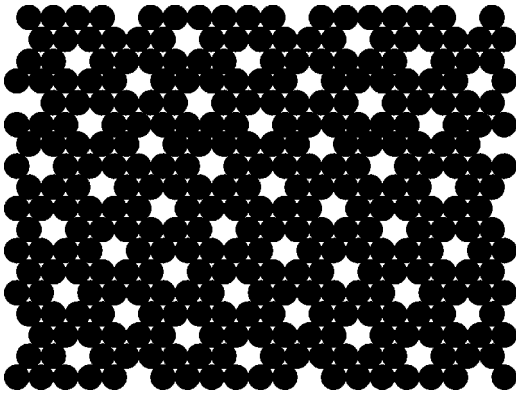


FIG. 11. Periodic chiral pattern of vacancies in the triangular lattice, representing the maximum vacancy concentration under the constraint of no vacancy pairs closer than fourth neighbors.

egory, whether increasing  $x$  across its range would encounter a disorder-order phase transition. The local jamming approximations Eqs. (5.11), (5.13), and (5.15) do not reveal such phase transitions. However, our planned subsequent studies employing more precise methods of analysis may reach different conclusions.

A final point is worth emphasizing to help place the families of lattice-based jammed packings in a larger geometric context. The results presented in Sec. IV above illustrate the fact that the lowest particle-density configurations for each of the “tri,” “bcc,” and “fcc” cases are still a large fraction of the perfect-lattice densities. With regard to local jamming at least, it has been demonstrated [17] that disk and sphere packings with arbitrarily low covering fractions  $\phi$  can be constructed. These low-density packings can be periodic, with arbitrarily large unit cells, but are not obviously the result of removing particles from an initial dense crystalline structure, such as the three types considered in the present study (tri, fcc, bcc). At present it is not known what the lowest attainable packing densities are for the collectively jammed and the strictly jammed criteria, whether periodic or otherwise.

#### ACKNOWLEDGMENTS

S.T. was supported by the Petroleum Research Fund as administered by the American Chemical Society and by the MRSEC Grant at Princeton University, NSF DMR-0213706. The authors thank Professor Robert Connelly for directing them to Ref. [17], and also thank Aleksandar Donev for invaluable discussions on several aspects of this paper. Finally, the authors thank Obioma Uche for producing the majority of the figures appearing in this paper.

#### APPENDIX

Let  $a$  stand for the collision diameter of contacting hard spheres arranged in a perfect bcc lattice. Consider then a fundamental cubic structural unit in that lattice consisting of a central sphere at the origin  $(0,0,0)$  of a Cartesian coordinate system, and its eight nearest neighbors at the positions  $(\pm 3^{-1/2}a, \pm 3^{-1/2}a, \pm 3^{-1/2}a)$  of the cube vertices. The edge length of this cube of neighbors,  $2 \times 3^{-1/2}a$ , exceeds  $a$  so that the eight neighbors are out of contact with one another.

Consider next a constant-volume uniaxial deformation of the cube into a rectangular solid. This will be implemented by multiplying  $z$  coordinates by a factor  $1 + \eta$ , while the  $x$  and  $y$  coordinates are multiplied by  $(1 + \eta)^{-1/2}$ . The resulting height  $h$  and base side length  $l$  of the rectangular solid will be

$$h = 2(1 + \eta)a/3^{1/2}, \quad (\text{A1})$$

$$l = 2a/3^{1/2}(1 + \eta)^{1/2}.$$

To avoid either of these distances becoming less than the collision diameter  $a$ , it is necessary to limit  $\eta$  to the range

$$3^{1/2}/2 \leq 1 + \eta \leq 4/3. \quad (\text{A2})$$

As a result of this uniaxial distortion, the common distance  $d(\eta)$  of all eight neighbors from the origin is the following function of  $\eta$ :

$$d(\eta) = 3^{-1/2}a[(1 + \eta)^2 + 2/(1 + \eta)]^{1/2}. \quad (\text{A3})$$

One easily verifies that over the range (A2) this expression attains its minimum at  $\eta=0$ , where in fact  $d=a$ . For any other  $\eta$  value in the range (A2),  $d$  exceeds  $a$ . Consequently, a uniaxial distortion of either sign breaks the eight contacts between the sphere at the origin and its neighbors. By extension, applying the same uniaxial distortion uniformly to an entire bcc lattice would break all of its sphere contacts, so that system would no longer be jammed. Consequently, the bcc crystal with rigid boundaries fails to meet the standard required for “strict jamming,” as defined in Sec. II above.

Note that this kind of argument cannot be applied to the close-packed triangular disk lattice or the fcc sphere lattice. Neither of these admit of a positive distortion range analogous to (A2), because the neighbors are already in contact with one another in the undistorted state, and in fact both lattices are strictly jammed.

[1] *Radiation Effects*, edited by W. F. Sheely, Metallurgical Society Conferences Vol. 37 (Gordon and Breach, New York, 1967).

[2] G. L. W. Hart and A. Zunger, *Phys. Rev. Lett.* **87**, 275508 (2001).

[3] S. Torquato and F. H. Stillinger, *J. Phys. Chem. B* **105**, 11 849 (2001).

[4] M. F. Thorpe, in *Physics of Disordered Materials*, edited by D. Adler, H. Fritzsche, and S. Ovshinsky (Plenum, New York, 1985).

- [5] C. Moukarzel and P. M. Duxbury, *Phys. Rev. E* **59**, 2614 (1999).
- [6] I. Avramov and R. C. R. Keding, *J. Non-Cryst. Solids* **272**, 147 (2000).
- [7] B. D. Lubachevsky and F. H. Stillinger, *J. Stat. Phys.* **60**, 561 (1990).
- [8] B. D. Lubachevsky, F. H. Stillinger, and E. N. Pinson, *J. Stat. Phys.* **64**, 501 (1991).
- [9] R. J. Speedy, *J. Phys.: Condens. Matter* **10**, 4185 (1998).
- [10] S. Torquato, T. M. Truskett, and P. G. Debenedetti, *Phys. Rev. Lett.* **84**, 2064 (2000).
- [11] L. Pauling, *J. Am. Chem. Soc.* **57**, 2680 (1935).
- [12] L. Pauling, *The Nature of the Chemical Bond* (Cornell University Press, Ithaca, NY, 1960), pp. 466–468.
- [13] A. R. Kansal, S. Torquato, and F. H. Stillinger, *Phys. Rev. E* **66**, 041109 (2002).
- [14] T. L. Hill, *Statistical Mechanics* (McGraw-Hill, New York, 1956), Chap. 7.
- [15] C. Domb, *Adv. Phys.* **9**, 149 (1960).
- [16] K. Huang, *Statistical Mechanics* (Wiley, New York, 1963).
- [17] K. Böröczky, *Ann. Univ. Sci. Budapest. Estvss Sect. Math.* **7**, 79 (1964).